The Simulation of a Bioinspired Variable Stiffness Sensor

Group 7

- **Avdhesh Gaur**
- **Erinma Okoro**
- **Sneh Ketankumar Shukla**

Paper Summary

Introduction

The paper, *Design of a Bioinspired Variable Stiffness Sensor*, introduces the design of force sensor systems inspired by whiskers, or vibrissae, as biological models. Vibrissae serve as a benchmark for detecting mechanical surface characteristics with exceptional adaptability. This work focuses on developing a tactile sensor system using simulation tools and control techniques.

Design Considerations

The Variable Stiffness Sensor (VSS) is modeled as a rigid body controlled during interaction with a contact surface. Control of the vibrissae model is achieved through two axial forces, governing its precise position and rotation. Resistance in the pivot, modeled as damping, is considered in the mechanical system. For simplicity, the model is reduced to a planar system, where the rigid vibrissa's position is controlled at the pivot point. Interaction forces between the surface and the vibrissa tip, driven by surface roughness, influence the dynamics. The mechanical model of the VSS can be seen below:

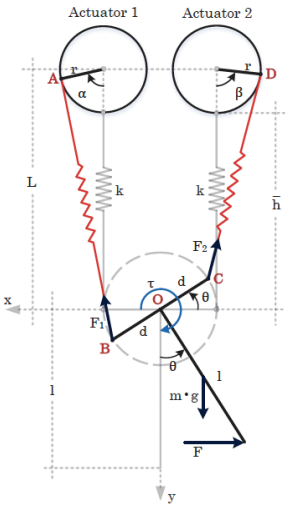

Objectives

The objectives of the paper—and by extension, this final project—include modeling the open-loop and PID-controlled closed-loop responses of the VSS system. Block diagrams representing these systems are shown below.

Block diagram of the variable stiffness sensor:

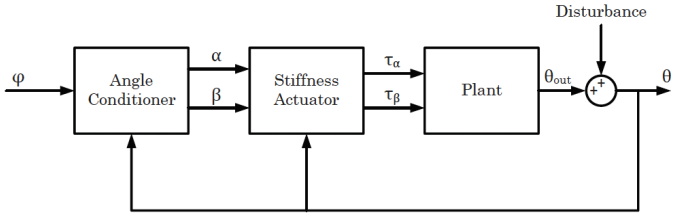

Block Diagram of the dynamic system in the state space:

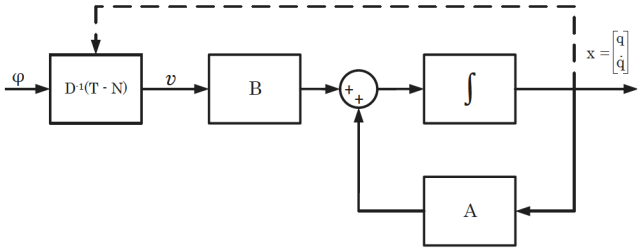

PID control model of the variable stiffness sensor:

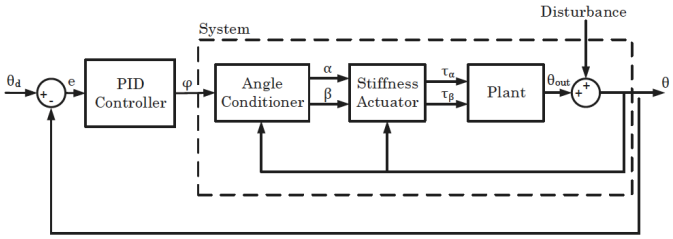

METHODOLOGY

A) System Model

Our model was developed following closely the dynamic equations and linearization methods outlined in the paper.

Dynamic Equations

I) Plant: The torque equilibrium approach is used with respect to the rotation of the actuators. The plant model is defined by the equations below:

$$\tau_O = \tau_\alpha + \tau_\beta.$$

where
T_o: Torque in the system
T_α: Torque produced by actuator 1
T_β: Torque produced by actuator 2

II) Stiffness Actuator: The torque T_o in the system is obtained through a course of calculations. The total torque produced by the system becomes:

$$\tau_O(q) = \hat{z}^T(\vec{OB} \times F_1 + \vec{OC} \times F_2),$$

$$S_1(\alpha, \beta, \theta) = \begin{bmatrix} d + r\sin(\beta(t)) - d\cos(\theta(t)) \\ -r\cos(\beta(t)) - \bar{h} - d\sin(\theta(t)) \\ 0 \end{bmatrix}$$

$$S_2(\alpha, \beta, \theta) = \begin{bmatrix} -d - r\sin(\alpha(t)) + d\cos(\theta(t)) \\ -r\cos(\alpha(t)) - \bar{h} + d\sin(\theta(t)) \\ 0 \end{bmatrix}$$

S_1 : Direction vector for force F1
S_2: Direction vector for force F2
F_1: Force applied to the device due to actuator 1
F_2: Force applied to the device due to actuator 2
with $q = [\alpha(t)\ \beta(t)\ \theta(t)]^T$

The dynamic model of the VSS is defined by:

$$\ddot{\theta}(t) = \frac{1}{J}\left(Fl\cos(\theta(t)) + mg\frac{l}{2}\sin(\theta(t)) + D_O\dot{\theta}(t) - \tau_O(q)\right)$$

III) Angle Conditioner: The purpose of the angle conditioner is to find a relationship between the input angle, φ, the actuator angles, α , β and the output angle θ, taking into consideration the initial angle, c. The relation between all angles is depicted in the condition below.

$$\begin{bmatrix} \alpha(t) \\ \beta(t) \end{bmatrix} = \begin{cases} \begin{bmatrix} \varphi(t) + c \\ c \end{bmatrix}, & \text{if } \varphi(t) \geq 0 \vee \theta(t) < 0 \\ \begin{bmatrix} c \\ \varphi(t) + c \end{bmatrix}, & \text{if } \varphi(t) \leq 0 \vee \theta(t) > 0 \\ \begin{bmatrix} c \\ c \end{bmatrix}, & \text{if } \varphi(t) = 0 \wedge \theta(t) = 0 \end{cases}$$

IV)Nonlinear Model Linearization: The dynamic model and angle conditioner equations given above are nonlinear. Therefore, it required some calculations to obtain the direct dynamic model from them which provided the torque resulting from the application of a certain angle *θ(t)*. The dynamic equation then was expressed as:

$$\ddot{q} = -D(q)^{-1}(T - H(q, \dot{q}) - C(q))$$

where D(q) is the inertia matrix, T is the generalized torque vector, H(q, q˙) is the Coriolis and centripetal force matrix and C(q) is the gravity matrix.

With the state vector being: $x = [q\ \dot{q}]^T$
This dynamic model in state variables was represented as a nonlinear space state system:

$$\dot{x} = f(x) + g(x)u$$

The subsequent control design was simplified using linear methods which is expressed below:

$$\ddot{q} = D^{-1}[T - N],$$

with: $N = H + C.$
The state vector is then presented in the form:

$$\begin{bmatrix} \dot{q} \\ \ddot{q} \end{bmatrix} = \begin{bmatrix} 0 & I \\ 0 & 0 \end{bmatrix} \begin{bmatrix} q \\ \dot{q} \end{bmatrix} + \begin{bmatrix} 0 \\ I \end{bmatrix} v,$$

with: $v = D^{-1}(T - N).$

With $q = [\alpha(t)\ \beta(t)\ \theta(t)]^T$ and $x = [q\ \dot{q}]^T$, the displacement of the system was represented in cartesian coordinates by six states. By the application of the general concept of feedback linearization, we have:

$$\dot{x} = \mathbf{A}x + \mathbf{B}v$$

V) Input: Input angles, ϕ. Open-loop input angles are modeled as sine waves with an amplitude of π and a period of 2 seconds.

VI) Disturbance: The disturbance is introduced as a pulse input, simulated using a pulse generator in Simulink.

VII) Desired output,θ_d: The desired output for the closed-loop system is created by combining three sine waves:

- **Wave 1:** Amplitude 0.1, Period 6.4 seconds.
- **Wave 2:** Amplitude 0.03, Period 3.2 seconds.
- **Wave 3:** Amplitude 0.12, Period 2 seconds.

VIII) PID Control: A PID block in Simulink was employed for closed-loop control. Initially, the article-provided values (K_p=0.545,K_i=0.474,K_d=0.157) were used but did not yield favorable results. After tuning, K_p=1, K_i=1.7, K_d=0.5 produced a satisfactory response.

IX) Output: Output angles, θ. The output angles are determined by displacement of the vibrissae due to applied forces and torques obtained from both the open loop and closed loop systems.

B) Model Parameters

After determining how the system was to be modelled, simulation parameters were extracted based on system requirements. However, some missing parameters necessitated contacting the paper's authors for clarification. The parameters obtained are enumerated below:

1. Vibrissa length, l = 0.03 m
2. Vibrissa mass, m = 0.0000354 kg
3. Spring length, h = 0.00515 m
4. Spring mass, M = 0.0000414 kg
5. Spring stiffness, k = 71N/m
6. Motor joint length, L = 0.01 m
7. Vibrissa shoulder radius, d = 0.0085 m
8. Actuator radius, r (r: L - h) = 0.00485 m
9. Damping coefficient at pivot O, Do = 0.0001
10. Moment of Inertia, $J = \frac{1}{3}*m*l^2$
11. Acceleration due to gravity, $g = 9.81 m/s^2$
12. Initial angle, c = 80 degrees
13. Force, F = 0.94N
14. Block A (6x6) Matrix A = [0 0 0 1 0 0; 0 0 0 0 1 0; 0 0 0 0 0 1; 0 0 0 0 0 0; 0 0 0 0 0 0; 0 0 0 0 0 0;]
15. Block B (6x1) Matrix B = [0; 0; 0; 1; 1; 1]

C) Additional Simulation Conditions

1. Subsystem Design: Due to system complexity, key components such as the angle conditioner, actuator, and plant were encapsulated in a Simulink subsystem for ease of access and management. This subsystem is easily accessed by double-clicking on it.

2. Open-Loop System Challenges:: Using parameter units as provided allowed the system to run initially, but it crashed at 0.07 seconds post-conversion to standard units. Reducing the step size did not resolve the issue. We proceeded to linearize the open system to address its stability issues.

D) Simulated Models

The simulation models were constructed in Simulink, guided by dynamic equations and linearization methods. Parameter definitions were managed in MATLAB files, and block diagrams from the objectives were used to structure the open-loop and closed-loop systems. Building the blocks directly in Simulink simplified tuning and adjustments during the process.

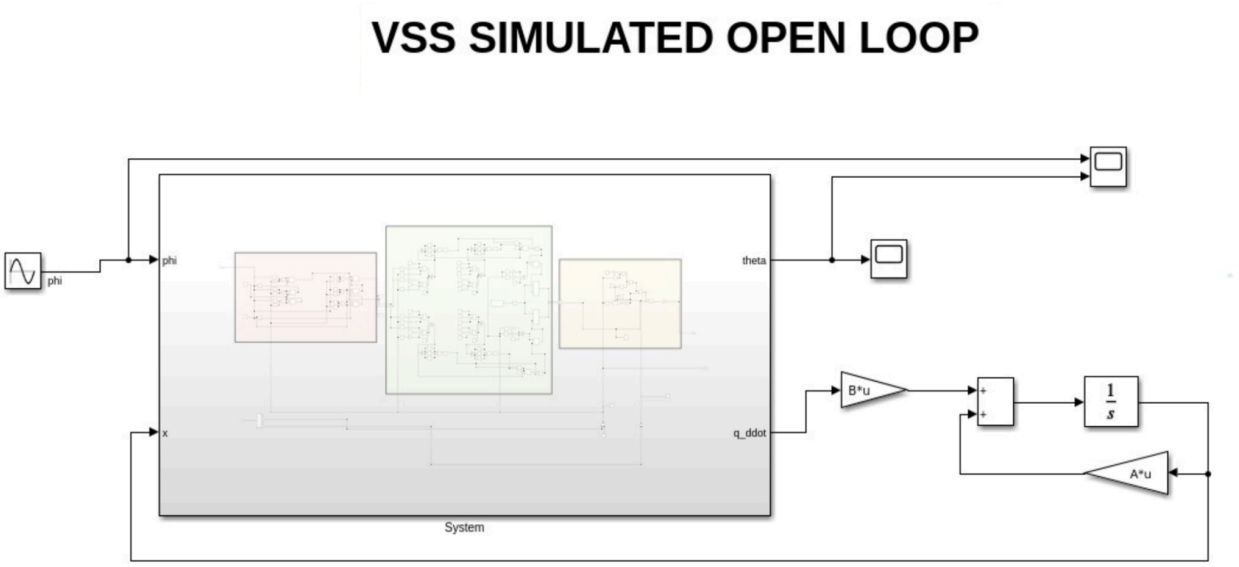

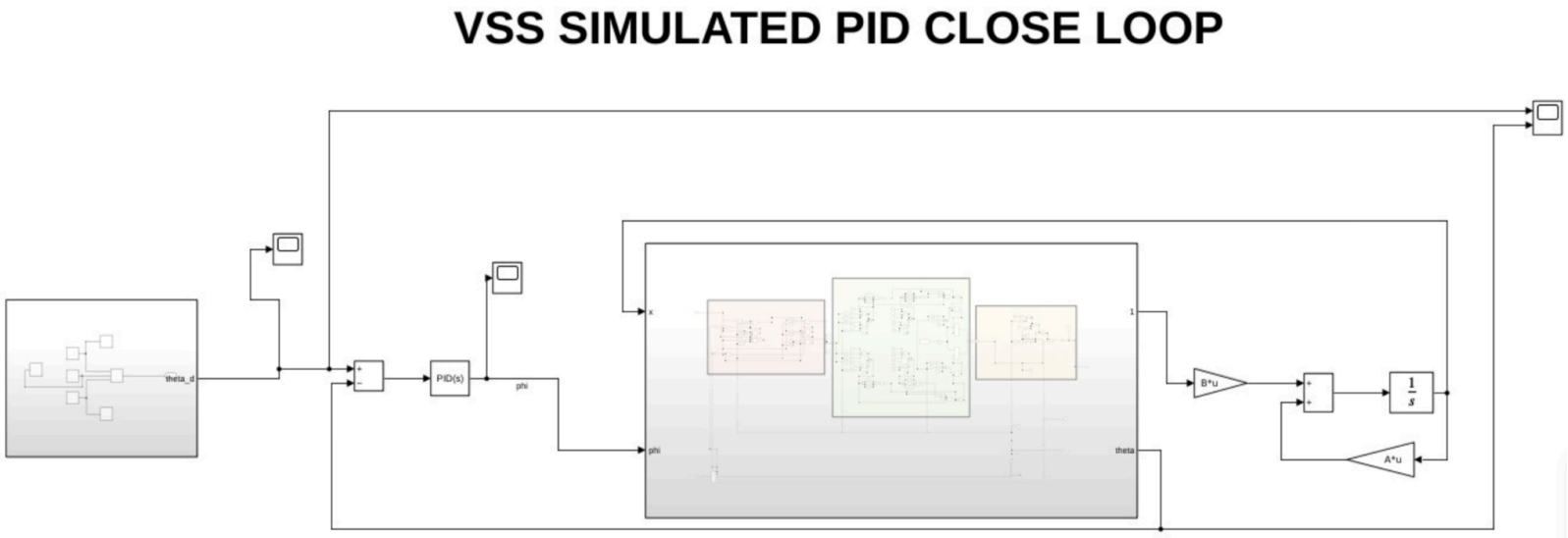

Simulation Results

A) Linearized Open Loop

I) Input and Output Signals: Simulated vs Reference Signal

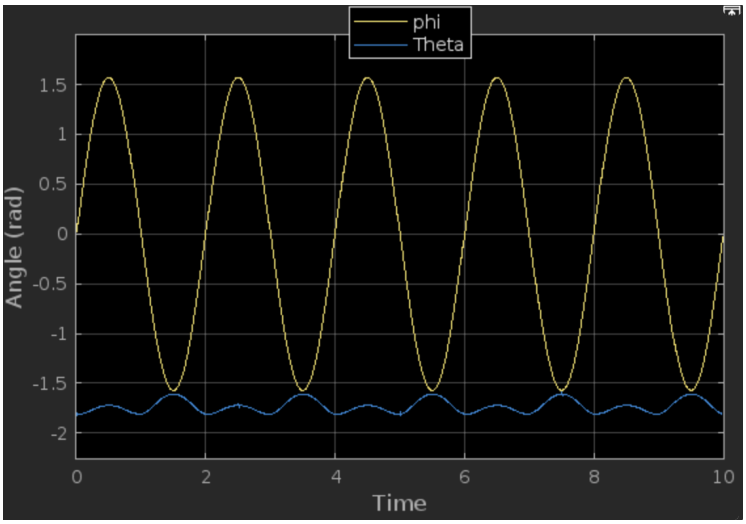

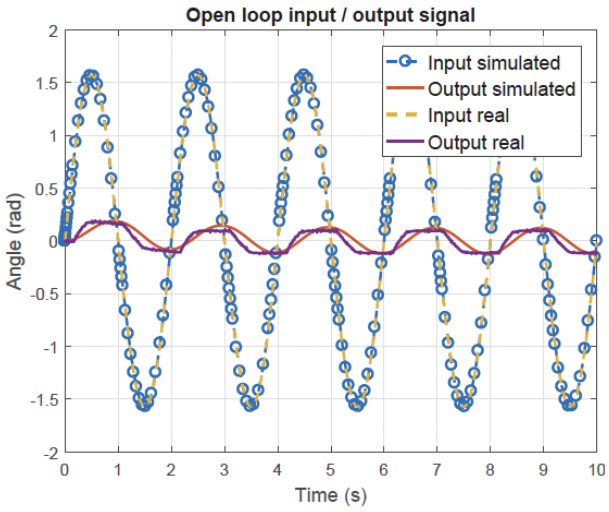

II) Output Signals: Simulated vs Reference Signal

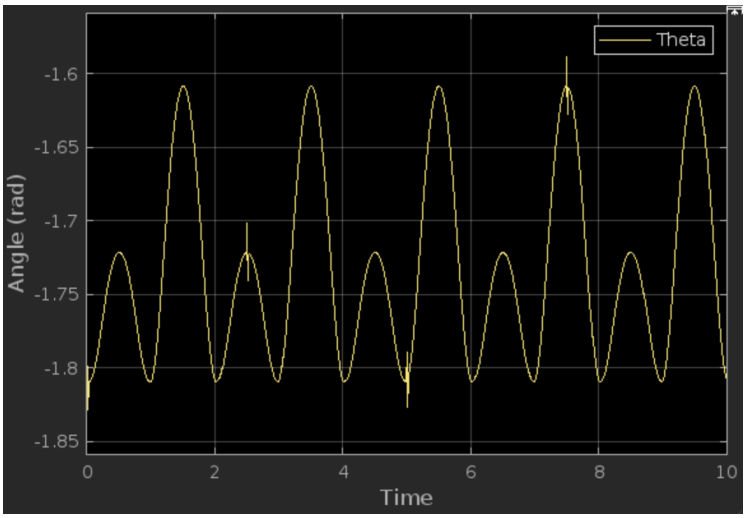

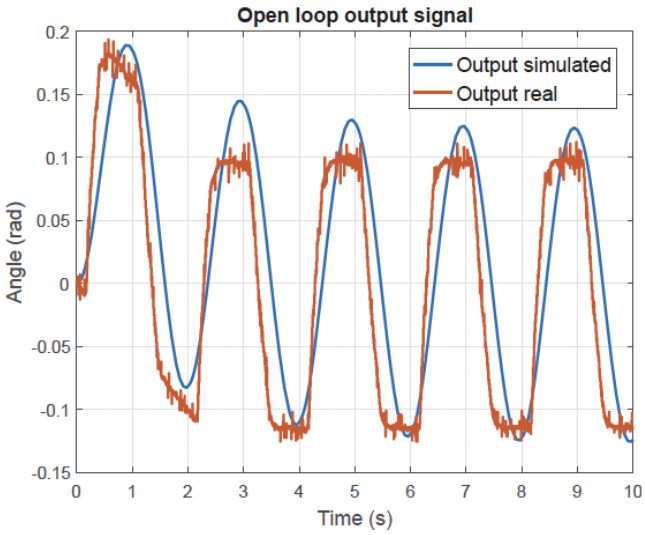

- Black background - Our simulated images
- White background - Reference simulated and real images

III) Result Analysis: In the open-loop system, the simulated and referenced input signals are identical. However, the simulated output signal is consistently lower than the referenced output signal. The referenced output signal has a mean of 0, similar to the input signals, whereas the simulated output signal has a mean of approximately -1.71 radians.

B) Closed Loop

I) Desired Output vs Output signals: Simulated vs Reference Signal

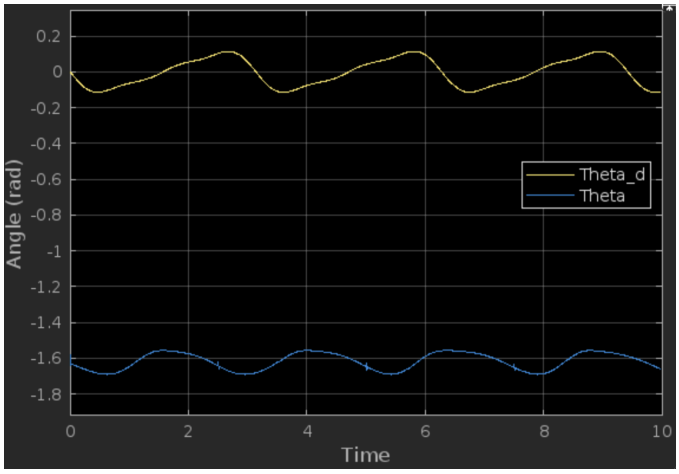

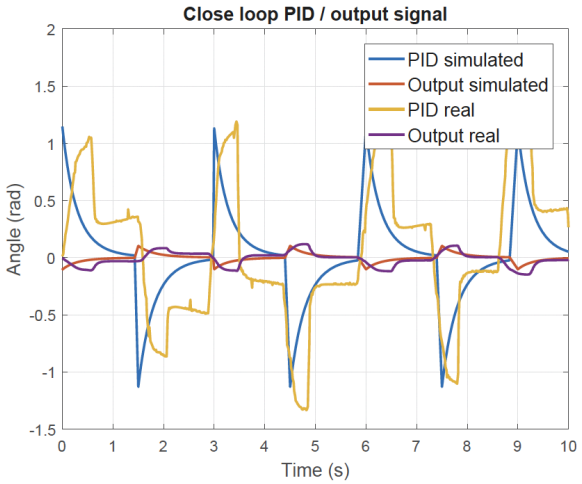

II) Torque signals: Simulated vs Reference Signal

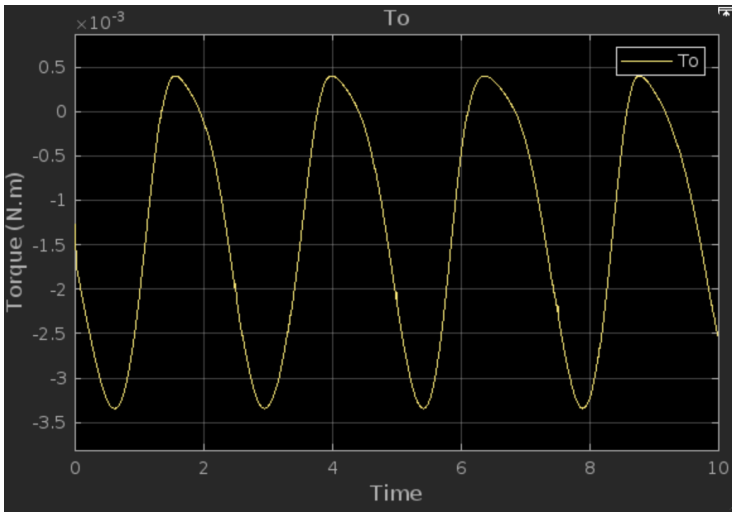

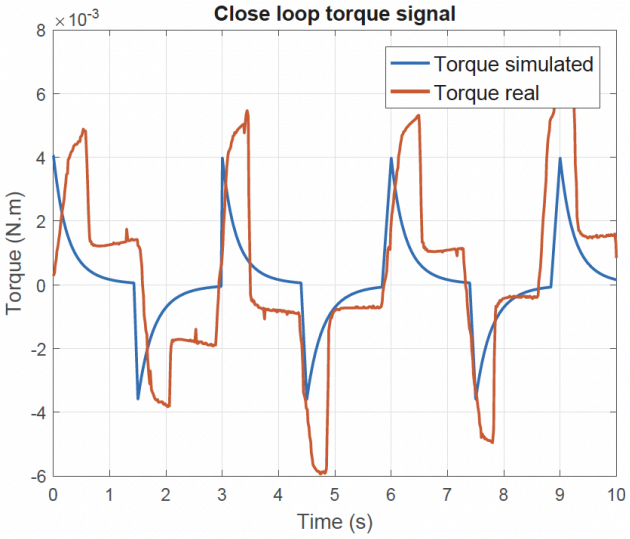

III) Result Analysis: Similarly, the simulated output signal in the closed-loop system is lower than the referenced output signal, though it retains some characteristics of the reference signal, although inverted. The simulated torque signal exhibits a peak-to-peak amplitude of about $4x10^{-3}$Nm, compared to that of the referenced signal is about 9 $x10^{-3}$ Nm.

Neither systems' response aligned with the results presented in the paper.

Developed Model Validation

While our simulated system responses differ from those documented in the paper, they successfully achieve the primary objectives of the Variable Stiffness Sensor (VSS) model.

Examining the mechanical model of the VSS used in this simulation (depicted in the first figure and highlighted further below), it is evident that the force F is directly proportional to the output response θ. Both the linearized open-loop and closed-loop systems were simulated with an applied force F of 0.94 N. When this force was reduced to 0 N, a corresponding decrease in the output response was observed.

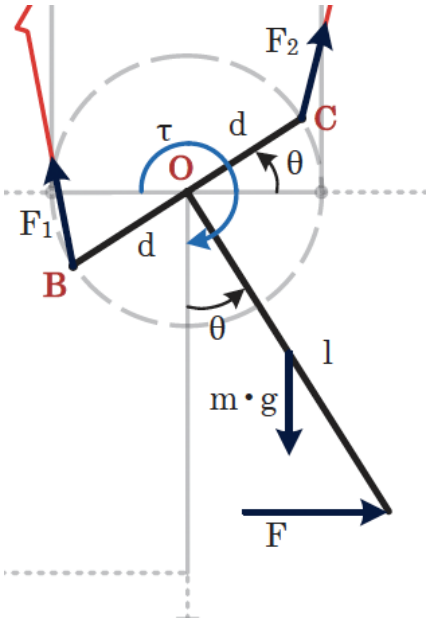

I) Open loop: 0.94N vs 0N

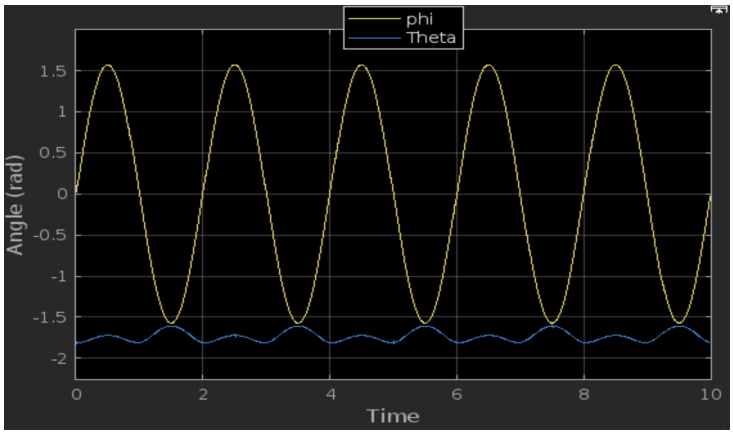

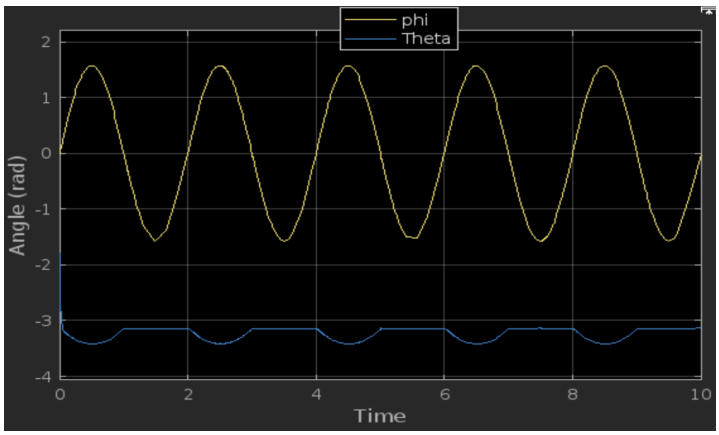

II) Closed loop: 0.94N vs 0N

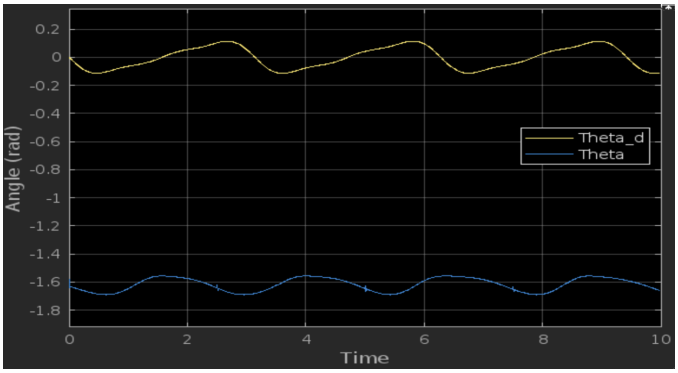

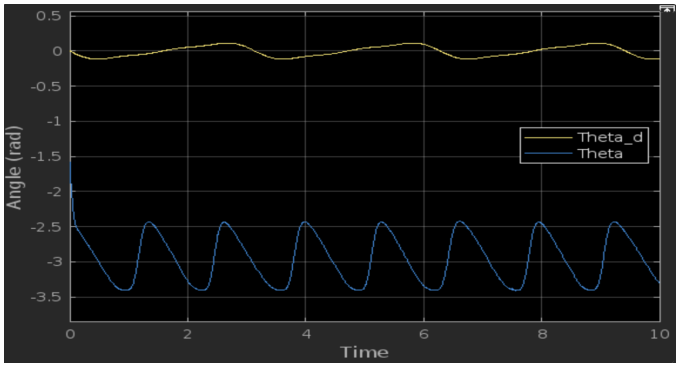

In the open-loop system, the mean output signal dropped from approximately -1.71 radians to about -3.3 radians when the applied force was zero. This behavior was similarly reflected in the closed-loop system, reinforcing the model's consistency with the principles described in the paper.

Although our model does not perfectly replicate the paper's results, it effectively demonstrates the functionality and behavior of the VSS model as outlined in the study. We believe this confirms the validity of the systems simulated for this project and highlights the relevance of this project to the objectives of the paper.

Conclusion

The methodologies outlined in the paper were diligently followed to design the systems as closely as possible to the original model. While the paper provided clear guidance, it appears that some critical details were not explicitly documented. The authors were gracious enough to respond to inquiries and shared relevant information available. They also mentioned incorporating deep learning techniques into their simulation, which could explain why the results did not perfectly replicate their model.

Despite these challenges, the developed model successfully captures the core functionality of the Variable Stiffness Sensor. This work demonstrates the sensor's ability to mimic whisker-like behavior, achieving the fundamental objective of exploring how vibrissae interact with and adapt to surface characteristics.